Electronic Supplementary Material (ESI) for Journal of Materials Chemistry A

Supporting Information

SiC nanocrystals as Pt catalyst supports for fuel cell applications

Rajnish Dhiman[a,b], Erik Johnson[c], Eivind M. Skou[b], Per Morgen[a], Shuang M. Andersen[b]

[a] Department of Physics, Chemistry and Pharmacy

University of Southern Denmark (SDU)

Campusvej 55 DK-5230 Odense M, Denmark

[b] Department of Chemical Engineering, Biotechnology and Environmental Technology

University of Southern Denmark (SDU)

Niels Bohr Alle 1, DK-5230 Odense M, Denmark

[c] Nano Science Center, Niels Bohr Institute,

University of Copenhagen

Universitetsparken 5, Copenhagen 2100, Denmark

1. Experimental Methods

1.1 Synthesis of SiC nanocrystals

SiC nanocrystals are synthesized through two different reactions using nanoporous carbon black (Vulcan® XC-72) as the carbon source with a particle size of 25 - 35 nm. The two reactions involved are (1) the solid phase reaction of carbon with molten silicon and (2) a reaction of carbon with *in situ* generated silicon monoxide vapors. In the solid phase reaction, silicon powder with the crystal sizes in the range 200 nm – 5 µm is uniformly mixed with carbon black in a 1:1 molar ratio with the help of a piston and mortar. The mixture is transferred into an alumina crucible and heated to a temperature of 1525 ˚C ± 25 ˚C in a tubular furnace (Lenton Thermal Designs Ltd.) for 6h in an argon flow of 250-300 ml/min. The furnace is heated and cooled at the rate of 5 °C/min. In the second method, the SiO vapors are generated by heating a uniform 1:1 molar mixture of silicon and silica powder at 1450 ℃. The carbon black is placed next (downstream) to this mixture in the alumina crucible. The furnace is heated to a temperature of 1450 ℃ for 12-15 h in an argon flow of 250-300 ml/min[28].

The SiC samples were characterized by X-ray diffraction (XRD), using a Siemens Diffractometer D5000, and imaged in a Hitachi S-4800 scanning electron microscope (SEM). The morphology, structure, defects, and crystal phases of individual SiC nanocrystals were examined by transmission electron microscopy (TEM) using a Philips CM20 instrument operated at 200kV. The confirmation of the silicon carbide character is also done using a Raman microscope from Dilor, using the 456 nm Ar-ion laser line, and with X-ray photoelectron spectroscopy (XPS) using a SPECS PHOIBOS 100 system®.

1.2. Platinum loading of SiC nanocrystals

1.2.1 Acid treatment of SiC nanocrystals

Acid treatment was performed by mixing SiC nanocrystals (catalyst supports) with concentrated acids [29,24]. SiC supports were taken in a flask and mixed with an acidic solution of 8.0 M HNO_3 (SIGMA-ALDRICH) and 7.5 M H_2SO_4 (BDH PROLABO), diluted from 65% HNO_3 (25 ml), 96% H_2SO_4 (20 ml) and distilled water (3 ml), which makes a total volume of about 48 ml. This solution containing the support material is sonicated for 10 min to ensure the dispersion of the SiC materials. After the sonication, the solution along with the material is transferred to a spherically bottomed flask immersed in a silicone oil bath. This was followed by refluxing the reaction mixture at 60 ℃ for 3h with constant stirring using a

magnetic stirrer. After the surface treatment, the SiC materials were transferred to a beaker and separated from the acids, first by suspension and then in a centrifuge with the repeated addition of distilled water until the pH value of 7.0 is reached.

1.2.2 Deposition of Pt nanoparticles on SiC supports

Platinum loading of SiC was carried out after the surface treatment by using potassium tetra-chloroplatinate (K_2PtCl_4) (Pt%: 46.78, ChemPur) as the metal precursor by using the polyol method [29,24]. A solution of ethylene glycol (EG) (99.5%,) and distilled water was made in the volume ratio of 9: 1 for EG and H_2O respectively. 50 mg of SiC was taken in a round spherically bottomed flask and an aliquot of 15 ml of solution. The amount of K_2PtCl_4 in the precursor solution corresponds to the targeted loading of the substrate. The solution containing SiC was sonicated again for 2-3 min to ensure the dispersion of SiC material into the solution and the flask was then put on a hot plate. The precursor solution was added drop wise to the flask. The reduction reactions were performed under reflux conditions at 125 ℃ for 3h with constant stirring. After the reaction, the SiC with Pt nanoparticles was separated from the ethylene glycol solution in the centrifuge and washed with distilled water 5-7 times. The masses of SiC material were monitored carefully throughout the entire process. Special attention was given not to lose material during separations at any stage. The metal loading as calculated from the masses of starting SiC materials, and the final Pt/SiC ratio, was expected to be in the range of 20-25%. TGA of Pt/Vulcan gives a value of 22% loading of Pt by weight. However, TGA cannot be used to determine the Pt loading of Pt/SiC, since SiC does not decompose within operation temperature range of TGA (~ 1000 ℃).

1.3. Electrochemical measurements

A conventionally used three-electrode setup was used for the measurements of the electrochemically active surface area of the supported catalyst samples by hydrogen adsorption / desorption. A suitable amount of catalyst was sonicated in Milli Q water for 15 min, and was directly dispersed on a gold electrode (2 x 6 mm^2) or polished glassy carbon electrode (diameter 5 mm) according to the targeted amount of Pt on electrode, followed by drying with a heating lamp in open air. This prepared electrode was used as the working electrode, while a reversible hydrogen electrode (RHE) from Gaskatel GmbH, Germany was used as the reference electrode (RE) and a platinum wire of 0.3 mm thickness wound with 40 windings constituting around a 3mm diameter was used as the counter electrode (CE). A 0.5 M aqueous $HClO_4$ solution (purged with a steady Ar flow for more than 45 min) was used as electrolyte. The system was controlled by an electrochemical workstation (IM6, ZAHNER). All the measurements were recorded for 2 CV cycles between 0.02 and 1.4 V, vs. RHE, at a scan rate of 50 mV/s, after initially running 20 trial cycles for electrochemical cleaning of the working electrode. The data was treated in OriginPro 8.5® (Originlab, USA). Hydrogen adsorption due to the gold electrode background was subtracted during the data treatment.

2. Mechanism of growth of SiC nanocrystals

The SiC nano crystals are grown by a solid phase reaction of a nano template of carbon (nano porous carbon black) with molten silicon, which is obtained by heating it above its melting point (1410 ºC). The reaction temperature is 1525 ℃ so that the silicon is in the molten form.

To the best of our knowledge, Larpkiattaworn *et al.*[27] is the only reported work studying the synthesis of nano-sized SiC in the temperature range of 1250 ℃ – 1350 ℃ by the solid phase reaction of silicon and carbon in vacuum and argon flow. But, surprisingly, they observed two competing synthesis routes, one through a gas–solid (SiO–C) reaction and the other through a solid phase (Si–C) reaction. These reactions are shown below:

$$\text{Si (liquid)} + \text{C (solid)} \rightarrow \text{SiC (solid)} \quad \text{(solid phase reaction)} \qquad (1)$$

$$\text{SiO (gas)} + 2\text{C (solid)} \rightarrow \text{SiC (solid)} + \text{CO (gas)} \quad \text{(gas-solid reaction)} \qquad (2)$$

They proposed that SiO is generated by the reaction of Si with the ambient oxygen.

However, in the present study, only the solid phase reaction (Si–C) is witnessed to produce SiC nanocrystals by a direct reaction of Si with C and this conclusion is based on the observation that more than 95% (by weight) of the reactants are recovered as product after the reaction, which would never be possible by assuming both reactions as parallel synthesis routes (explained later in the section).

Figure S1 shows a graph of the fraction of the product obtained to the amount of reactants used with respect to the percentage of product obtained from the solid phase reaction, where the rest of the product is obtained by the gas solid reaction. These calculations have been made by considering both reactions (1) & (2). If we assume that 90% of the obtained product (SiC) is synthesized through the solid phase reaction and the rest of it (10%) is synthesized by the gas solid reaction, then the maximum amount of SiC obtained will only be 91% of the starting reactant mixture (silicon and carbon) and the end product will contain 6.5% unreacted silicon.

Figure S1 shows all the possibilities and it predicts that the end product will always contain a significant amount of unreacted silicon if the reaction follows the gas-solid reaction, with the only exception being a 100% solid phase reaction. We have recovered more than 95% of the reactants; moreover we could not find unreacted carbon or unreacted silicon (as evident from XRD, Raman and XPS characterizations). The product has been checked for unreacted carbon by heating to 650 ºC in open air. It has also been checked for unreacted amorphous Si by etching with conc. HNO_3 and HF. Thus, these observations prove that the solid phase reaction is the synthesis route for nanocrystals in the present work. The 5% (approx.) loss may have occurred due to the combination of some errors in measurements or handling and some loss of silicon as SiO vapors, since the outer layers of silicon generally get oxidized and this oxide may react with silicon to form SiO vapor.

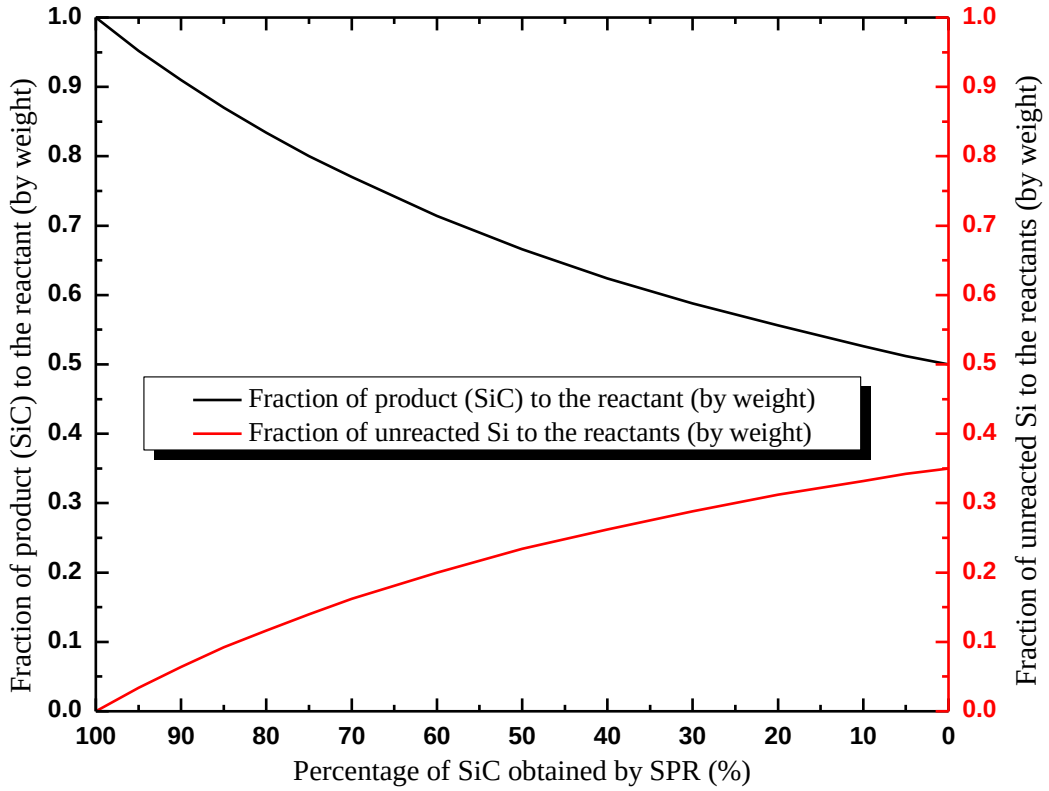

Figure S1. Plot of the fraction of product (SiC) to the reactant, and the fraction of unreacted Si to the reactant, versus the percentage of SiC obtained by the solid phase reaction (the rest of SiC is assumed to be formed by the gas-solid reaction).

The growth mechanism of SiC nanocrystals is believed to occur through the diffusion of the molten silicon through the nanoporous carbon powder. The porous carbon nano-clusters are contacted by the silicon melt from all directions, covering them completely and pulling the silicon into the pores of these carbon particles to start the nucleation of SiC crystals. A possible reason for our observations differing from those of Larpkiattaworn *et al.*[27] is the higher temperature of the present synthesis since the increase in temperature enhances the reaction rate. The diffusion of silicon in the porous carbon is fast in its molten form, leaving no time for the generation of SiO vapors. The growth rate has been observed to increase with temperature [27].

3. SEM and TEM images

Figs. S2 and S3 shows some SEM and TEM images of SiC-SPR and SiC-NS and their Pt deposited counterparts (Pt/SiC_SPR and Pt/SiC-NS).

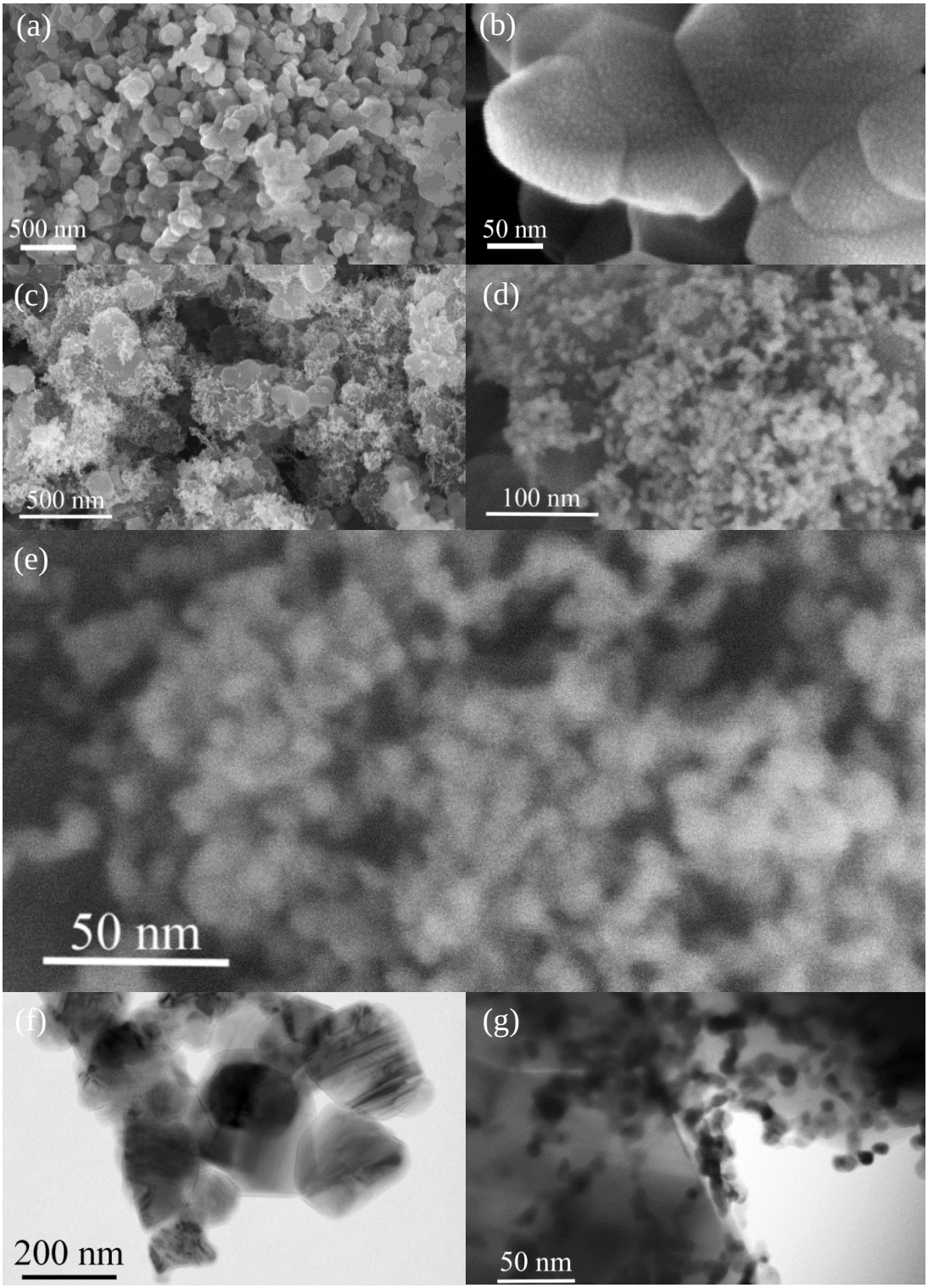

Fig. S2(a) & (b) are SEM images of SiC-SPR, (c), (d) and (e) are SEM images of Pt/SiC-SPR. (f) & (g) are TEM images SiC-SPR and Pt/SiC-SPR respectively.

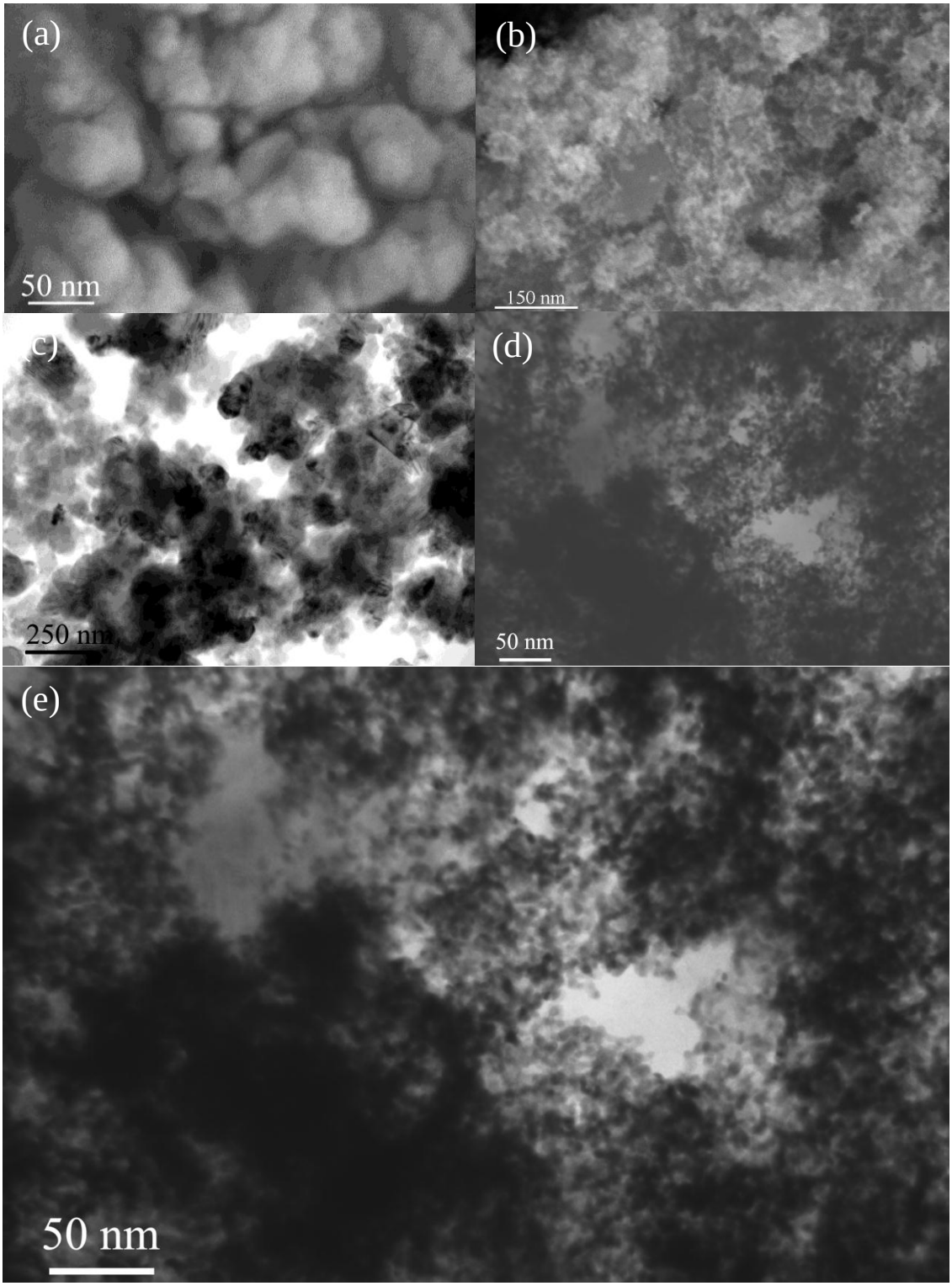

Fig. S3(a) SEM image of SiC-NS, S3(b) SEM image of Pt/SiC-NS, S3(c) TEM image of SiC-NS and (d) and (e) are TEM images of Pt/SiC-NS.

4. XPS analysis

Figure S4 show the XPS survey spectra of SiC nanocrystals. These spectra mainly show the presence of silicon, carbon, and oxygen, in the sampled volume.

Table S1 gives the elemental composition of the two types of SiC nanocrystals. The sample SiC-NS shows double the amount of oxygen than the SiC-SPR. As can be seen from the SEM and TEM images (Figs. 3, 4, S2 & S3), the SiC-NS have small particle sizes thus giving a higher surface area, which helps in adsorbing oxygen. Moreover the reaction time for SiC-NS is 2.5 times longer than the SiC-SPR, which increases the chances of oxygen uptake during synthesis. Apart from Si, C, O and N, a small fluorine peak (< 1%) is also found in SiC-SPR because the sample was checked for some unreacted amorphous silicon by etching with HF and HNO_3. No crystalline unreacted silicon had been found in XRD. The measurement after etching did not show any unreacted silicon in the sample.

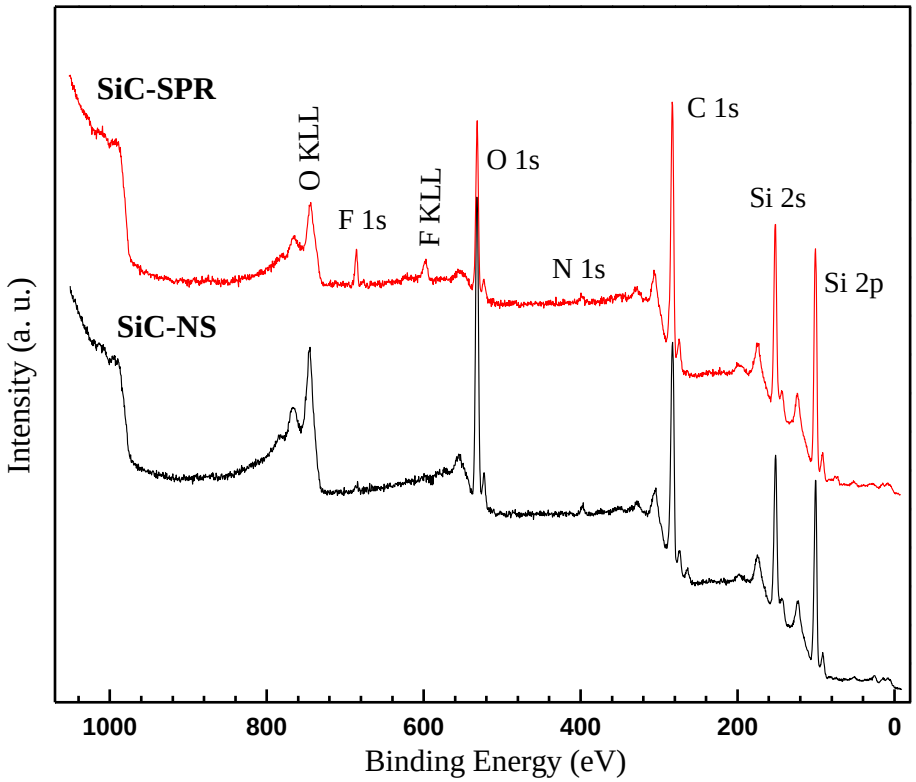

Figure S4. XPS Survey spectra of the SiC nanocrystals.

The comparison of relative elemental composition (Table S1) of both the samples with their acid treated and platinized counterparts shows that the acid treatment reduces the amount of silicon, enhances the relative amount of carbon, while the amount of oxygen increases in SiC-SPR and it remains the same in SiC-NS. As, discussed in main text, this may have happened due to the combined effect of etching of surface oxide on SiC and addition of surface groups during acid treatment. The platinization of the acid treated substrates significantly reduces the amount of carbon detected (in comparison to amount of silicon) and this may be due to a shadow effect. After loading Pt over SiC, the area of open and visible SiC surface is reduced

(as can be seen in the SEM/TEM images). The size of the Pt particles is 5-8 nm. Since the inelastic mean free path (IMFP) of electrons is directly proportional to the square root of kinetic energy (KE), the IMFP of the emitted electrons from carbon should be lower than that corresponding to silicon. Electrons with higher KE may thus penetrate the spherical or thinner edges of Pt particles and may reach the analyzer. Thus the presence of Pt particles will affect the C-signal more than the Si-signal. This may be the reason for finding an apparently reduced amount of carbon after platinization.

Table S1. Elemental relative composition of the SiC nanocrystals, acid treated SiC and Pt loaded SiC. These values are based on the XPS spectra in Fig. S4 and Fig. 5 (in the article) and refer to the sampled volume.

Sample Name	Si/%	C/%	O/%	Pt/%	F/%	N/%
SiC-SPR	47.1	42.9	8.5	-	0.9	0.6
SiC-SPR acid treated	42.9	44.1	12.3	-	-	-
SiC-SPR acid treated and platinized	42.6	32.0	8.8	16.4	0.2	-
SiC-NS	41.6	41.4	16.2	-	-	0.8
SiC-NS acid treated	38.6	44.8	15.8	-	0.7	-
SiC-NS acid treated and platinized	32.6	29.5	17.8	20.1	-	-

Figure S5 shows the high resolution spectra and deconvolution of the individual C 1s and Si 2p regions for SiC-SPR and SiC-NS. The C1s spectrum of SiC-SPR is composed of three components with positions at 283.0, 285.1 and 286.3 eV. These peaks correspond to SiC, C-C and C-OH bonding respectively. The atomic percentage of each component based on peak deconvolution (Figure S5) can be seen from the Table S2. The Si 2p spectrum of SiC-SPR is deconvoluted into two peaks at 99.9 and 102.7 eV corresponding to SiC and SiO_2 (see Table S2). The table shows only a small amount (1.6 %) of SiO_2 bonding, which indicates that the sample is less oxidized and whatever oxygen (8.5%) as shown in Table S1 is bonded as C-OH. Thus, the small amounts of C-C and C-OH bonds may be due to the handling of the sample after synthesis, since the XPS is very sensitive to the surface contamination.

The peak deconvolution of SiC-NS is also similar to that of SiC-SPR with C1s showing peaks at 283.0, 285.0 and 286.1 eV corresponding to SiC, C-C and C-OH and C-N bonding. Unlike the Si 2p spectrum of SiC-SPR, the spectrum in SiC-NS shows three components with an addition of peak at 102 eV (3.1%). This sample shows 8.4 % of SiO_2 bonding (SiC-SPR have 1.6 %), which is also consistent with the amount of oxygen in both samples as shown in Table S1. SiC-NS also shows a slightly higher amount of C-C bonds and also a peak at 285.9 eV, than SiC-SPR. The peak at 285.9 in SiC-NS might be due to the combination of C-OH and C-N, since Si 2p also shows a Si (N,O) peak with 3.1% at 102.0. Thus, the component at 102.0 eV in SiC-NS shows that a small amount of silicon oxynitride is also formed along with the silica layer (103 eV). The nanoporosity of the precursor (carbon black) and the synthesized sample, along with the longer synthesis time (2.5 times longer than for SiC-SPR), increase the

chances of adsorption of oxygen and nitrogen and may thus be responsible for a relatively higher amount of SiO_2 and traces of N bonded to SiC in this case.

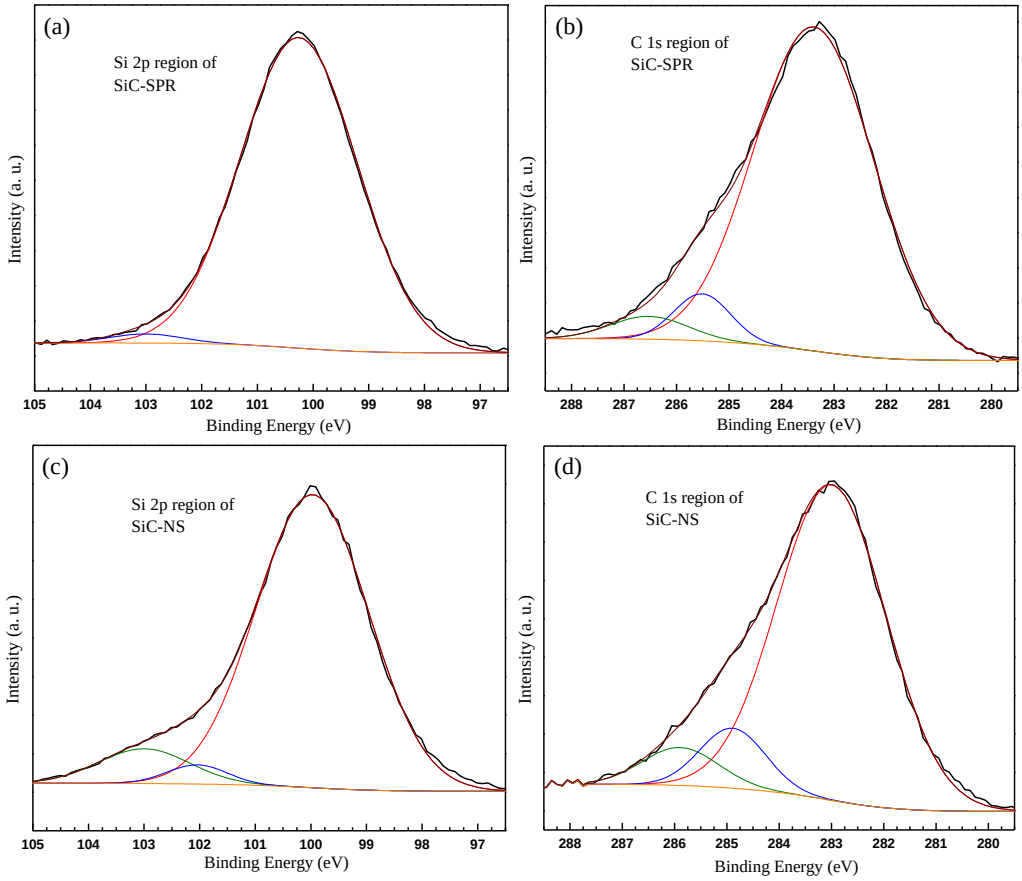

Figure S5. The deconvoluted (a) Si 2p and (b) C 1s peaks of SiC-SPR, and (c) Si 2p and (d) C 1s peaks peaks of SiC-NS.

Table S2. Peak deconvolution of Si 2p and C 1s regions of SiC nanocrystals based on Fig. S5

Sample name	Peak regions	Bond type	Position	Relative %
SiC-SPR	C 1s	SiC	283	88.3
		C-C	285.1	6.7
		C-OH	286.3	5.0
	Si 2p	SiC	100	98.4
		SiO_2	103	1.6
SiC-NS	C 1s	SiC	283.0	83.5
		C-C	284.9	9.5
		C-OH & C-N	285.9	7.0
	Si 2p	SiC	100.0	88.5
		SiO_2	103.0	8.4
		Si(N,O)	102.0	3.1

Figures S6 and S7 shows the C 1s, Si 2p and Pt 4f peak deconvolution in high-resolution spectra of Pt/SiC-SPR and Pt/SiC-NS respectively. The peak deconvolution of both the samples show the same components but with slightly differing amounts. The deconvolution of the C 1s spectra for the platinized samples also show three components due to SiC, C-C and C-OH bonds (similar to the un-platinized samples). The C-C component either remains with the same intensity or decreases while there is a slight increase in the C-OH component, after platinization. This means that un-reacted C is going off with acid treatment along with the addition of some new surface groups such as C-O or C-OH on the SiC particles and they are also retained after platinization, since the analysis of acid treated SiC samples shows an increase in the amount of C and O (See Tables S1 and S3).

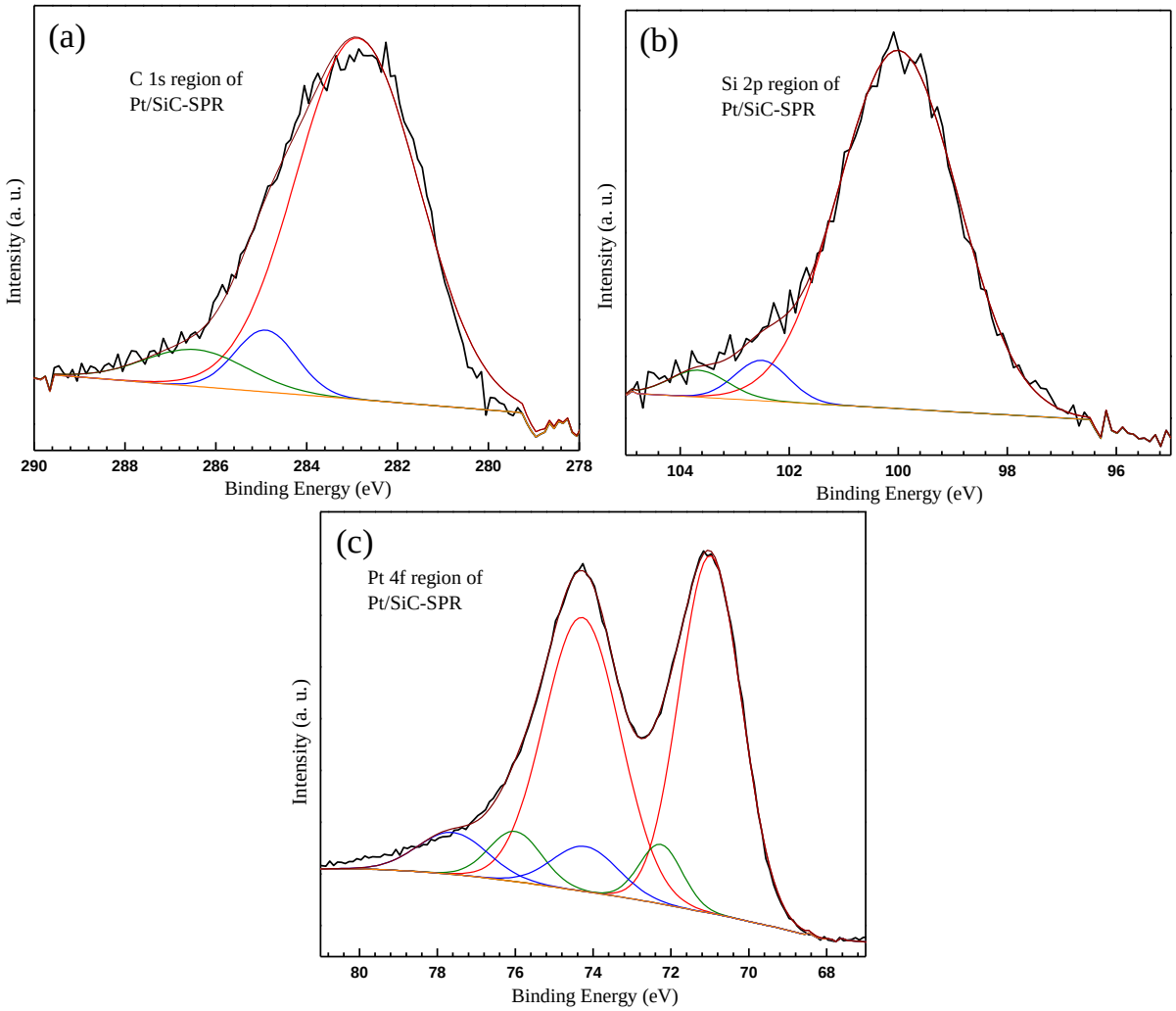

Figure S6. The deconvoluted (a) C 1s (b) Si 2p and (c) Pt 4f peaks of Pt/SiC-SPR.

The Si spectra after Pt deposition is composed of three peaks corresponding to SiC, SiO_2 and a third component at around 102 eV which may correspond to the surface groups (as seen in both samples). The acid treatment of the substrates was done to introduce oxygen surface groups. These surface groups are well known[32, 33] to help anchor the Pt particles on carbon supports, during the reduction of precursor solution to Pt, and thus to enhance the dispersion of platinum particles over the substrate. The Pt 4f peak is generally a doublet due to spin orbit

splitting and consists of 4f (7/2) at 71.1 eV and 4f (5/2) at 74.4 eV [34]. Deconvolution of the Pt 4f peaks result in three doublets marked Pt(0), Pt(II) and Pt(IV) in Figs. S6 & S7. The most intense peak at 71.1 (4f (7/2)) can be attributed to metallic Pt, while the less intense peaks can be ascribed to +2-valent and +4-valent Pt as in PtO and PtO_2 [35].

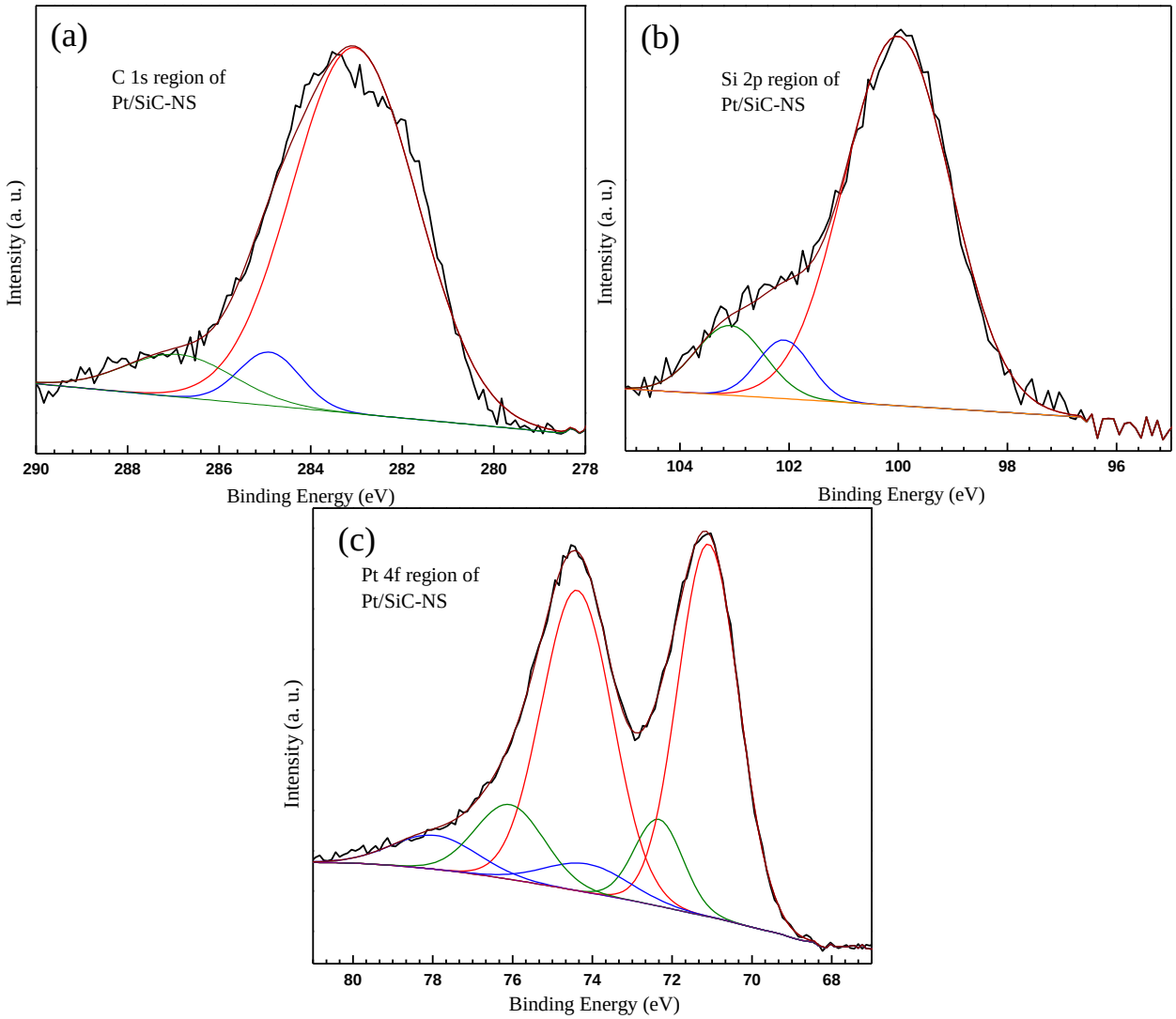

Figure S7. The deconvoluted (a) C 1s (b) Si 2p and (c) Pt 4f peaks of Pt/SiC-NS.

Table S3. Peak deconvolution of Si 2p, C 1s and Pt 4f regions of Pt/SiC (based on Fig. S6 and S7).

Sample name	Peak regions	Bond type	Position	Relative %
Pt/SiC-SPR	C 1s	SiC	282.9	86.0
		C-C	285.0	7.1
		C-OH, C-N	286.8	6.9
	Si 2p	SiC	99.9	94.1
		SiO_2	103.5	1.8
		Si (N,O), some surface groups	102.4	4.1
	Pt 4f	Pt(0) I (7/2)	70.9	41.2
		Pt(0) II (5/2)	74.2	38.0
		Pt(2) I (7/2)	72.2	4.7
		Pt(2) II (5/2)	72.2	5.9
		Pt(4) I (7/2)	74.4	5.0
		Pt (4) II (5/2)	77.7	5.3
Pt/SiC-NS	C 1s	SiC	283.0	85.3
		C-C	284.9	6.1
		C-OH, C-N	286.9	8.6
	Si 2p	SiC	100.0	83.4
		SiO_2	103.3	10.1
		Si (N,O), some surface groups	102.1	6.5
	Pt 4f	Pt(0) I (7/2)	71.0	39.0
		Pt(0) II (5/2)	74.4	36.2
		Pt(2) I (7/2)	72.3	7.1
		Pt(2) II (5/2)	75.9	8.7
		Pt(4) I (7/2)	74.2	4.1
		Pt (4) II (5/2)	77.9	4.9